



LAWRENCE
LIVERMORE
NATIONAL
LABORATORY

Energetic Electrons Driven in the Polarization Direction of an Intense Laser Beam Incident on a Solid Target

J. Seely, L. Hudson, N. Pereira, C. Di Stefano, C. Kuranz, R. Drake, H. Chen, G. J. Williams, J. Park

January 16, 2015

High Energy Density Physics

Disclaimer

This document was prepared as an account of work sponsored by an agency of the United States government. Neither the United States government nor Lawrence Livermore National Security, LLC, nor any of their employees makes any warranty, expressed or implied, or assumes any legal liability or responsibility for the accuracy, completeness, or usefulness of any information, apparatus, product, or process disclosed, or represents that its use would not infringe privately owned rights. Reference herein to any specific commercial product, process, or service by trade name, trademark, manufacturer, or otherwise does not necessarily constitute or imply its endorsement, recommendation, or favoring by the United States government or Lawrence Livermore National Security, LLC. The views and opinions of authors expressed herein do not necessarily state or reflect those of the United States government or Lawrence Livermore National Security, LLC, and shall not be used for advertising or product endorsement purposes.

Energetic Electrons Driven in the Polarization Direction of an Intense Laser Beam Incident on a Solid Target

J. F. Seely,¹ L. T. Hudson,² N. Pereira,³ C. A. Di Stefano,⁴ C. C. Kuranz,⁴ R. P. Drake,⁴ Hui Chen,⁵ G. J. Williams,⁵ and J. Park⁵

¹Artep Inc., 2922 Excelsior Springs Court, Ellicott City MD 21042, USA

²National Institute of Standards and Technology, Gaithersburg MD 20899, USA

³Ecopulse Inc., P. O. Box 528, Springfield VA 22152, USA

⁴University of Michigan, Ann Arbor MI 48109, USA

⁵Lawrence Livermore National Laboratory, Livermore CA 94551, USA

Abstract

Experiments were performed at the LLNL Titan laser to measure the propagation direction of the energetic electrons that were generated during the interaction of the polarized laser beam with a solid target. The target consisted of a central irradiated wire, two wires positioned above and below the irradiated wire in the vertical direction of the polarization of the incident laser beam, and two wires positioned on the sides of the irradiated wire in the horizontal direction, perpendicular to the polarization direction. The irradiated wire, the vertical wires, and the horizontal wires were of three different materials, for example Ho, Gd, and Dy. The K-shell spectral lines from the three materials were recorded by a transmission crystal spectrometer on each laser shot. The relative intensities of the $K\alpha$ lines from the vertical and horizontal wires were measures of the fluence of energetic electrons driven in the polarization direction and in the

perpendicular direction, respectively. The gap between the irradiated wire and the vertical and horizontal wires was varied on sequential laser shots, and the intensities of the $K\alpha$ lines were a measure of the angular distribution of the energetic electrons propagating from the irradiated wire. It was found that the fluence of energetic electrons was larger in the vertical direction of the polarization as compared to the perpendicular (horizontal) direction. This implies energetic electrons are preferentially driven in the direction of the intense oscillating electric field of the incident laser beam in agreement with the multiphoton inverse Bremsstrahlung absorption process.

Keywords: Multiphoton inverse Bremsstrahlung absorption, laser-plasma interaction, relativistic electron propagation.

PACS: 52.38.Kd, 52.38.Ph, 52.70.La; 32.30.Rj.

High Energy Density Physics, 1/6/2015.

I. Introduction

Soon after the invention of the laser it was realized that with increasing laser intensity, atoms would be quickly ionized and the resulting free electrons would be accelerated to relativistic energies during a single cycle of the oscillating electric field of the laser beam [1]. From a classical physics point of view, the quiver energy of the oscillating electron is converted to directional energy during a collision with a nucleus [2]. From a quantum mechanical viewpoint, as illustrated schematically in Fig. 1 the electron absorbs multiple laser photons during the collision with a nucleus, the inverse of Bremsstrahlung emission, and the process was named multiphoton inverse Bremsstrahlung absorption (MIBA) [3]. The rate of energy increase is the product $\epsilon_q v_{\text{eff}}$ where $\epsilon_q = e^2 E^2 / 2m\omega^2$ is the quiver energy, v_{eff} is the effective collision frequency with the nucleus, E is the strength of the electric field having oscillation frequency ω , e is the electron charge, and m is the relativistic electron mass [4]. In the classical limit of small \hbar , the reduced Planck constant, the quantum and classical expressions for the collision frequency agree except for a numerical factor of order unity [3].

A signature of the MIBA process is that the highest probability for multiphoton absorption occurs when the electron propagates perpendicular to the laser beam and in the polarization direction of the electric field after the collision with the nucleus [3]. While other laser-plasma interaction processes, such as the ponderomotive force and in the case of oblique incidence the resonance absorption and other processes, may act to accelerate electrons in the laser propagation direction and to expel electrons from the focused laser volume in all directions [5], in the case of normal incidence no process

other than MIBA selectively accelerates electrons in the polarization direction of the electric field.

The selective acceleration of electrons in the polarization direction during the interaction of a normal-incidence laser beam with a solid target was first observed in a qualitative sense during experiments at the LULI laser facility [6]. A plane-polarized, femtosecond laser beam having 10^{20} W/cm² intensity and 27 MV/μm electric field strength was focused onto a metal wire (gadolinium or tungsten) that was embedded in the surface of an aluminum target, and MeV electrons were generated in the focal spot and propagated into the irradiated wire along the direction of the laser beam and also laterally to an embedded spectator wire of a different material (dysprosium or hafnium). The energetic electrons created 1s vacancies in both the irradiated and spectator wires, and the resulting time integrated K-shell spectra from the two different wire materials were recorded by a transmission crystal spectrometer. The ratio of the K-shell emissions from the irradiated and spectator wires is a measure of the relative numbers of energetic electrons propagating in the forward direction of the laser beam and perpendicular to the laser beam. It was observed that more numerous energetic electrons were driven perpendicular to the laser beam than along the laser beam. In addition, it was observed that more numerous energetic electrons were driven in the polarization direction of the incident laser beam than in the perpendicular direction.

The present paper describes experiments utilizing laser-irradiated targets that are optimized for the quantitative study of the angular distribution of the energetic electrons propagating in the polarization direction and perpendicular to the polarization direction of the incident laser beam. The experiments were performed at the Titan laser facility at

Lawrence Livermore National Laboratory. The Titan beam was incident normal to the face of the target shown in Fig. 2, and the electric field of the laser beam was plane-polarized in the vertical direction. The target was composed of a central irradiated wire that was positioned in a hole that was perpendicular to the face of a 3 mm aluminum cube. Arrayed about the central wire were four spectator wires that were pressed into grooves in the surface of the cube, two vertical wires of one material and two horizontal wires of a different material. The spectator wire diameters and groove widths were 0.5 mm, the groove depth was 0.5 mm, and the axes of the spectator wires were 0.25 mm below the plane of the cube surface. The central irradiated wire also had 0.5 mm diameter, and the tip of the central wire was 0.25 mm below the plane of the cube surface and on the axes of the spectator wires. The tip of the irradiated wire and the ends of the spectator wires facing the irradiated wire were polished flat, and the separation gap between the ends of the spectator wires and the surface of the irradiated wire was varied on a sequence of laser shots. The laser beam was incident normal to the flat tip of the central wire (and to the face of the target shown in Fig. 2), and the focal spot was positioned at the center of the wire as enabled by orthogonal viewing cameras. Thus energetic electrons that were generated in the focal spot propagated into the irradiated wire and laterally across the open gap to the four spectator wires.

The central irradiated wire, the vertical wires, and the horizontal wires were of three different metals, for example Hf, Gd, and Dy as illustrated in Fig.2. The energetic electrons accelerated from the focal spot propagated into the three wire materials and generated 1s vacancies and K-shell spectra that were recorded by a transmission crystal spectrometer. The ratios of the $K\alpha$ spectral lines from the three materials are measures of

the relative numbers of energetic electrons propagating into the irradiated, vertical, and horizontal wires. In particular, the ratio of the K lines from the vertical and horizontal wires is a measure of the relative numbers of electrons propagating in the laser beam's polarization direction (vertical) and perpendicular to the polarization direction (horizontal).

The target is designed to mitigate laser shot-to-shot variations and other experimental uncertainties. For example, the emissions from the two vertical wires are summed as are the emissions from the two horizontal wires, and this mitigates small mis-positioning of the focal spot on the central wire: if the focal spot is off center toward a particular wire, then the emission from that wire would be stronger, the emission from the opposite wire of the same material would be weaker, and the sum of the emissions from the two wires would vary slowly with the off-center distance. In addition, the spectator wire materials are Gd and Dy which have similar atomic numbers (64 and 66) and material properties, and the small differences in material properties such as energetic electron stopping power and $K\alpha$ radiation generation tend to cancel out when taking the ratio of the emissions from the Gd and Dy wires.

II. Experimental Results

The experimental setup and the related study of the ranges of energetic electrons propagating from an irradiated wire through various materials to spectator wires are described in [7]. The Titan pulse typically had 100 J energy, 1 ps duration, 10 μm diameter focal spot, and 10^{20} W/cm^2 focused intensity. Two spectrometers were fielded, one having high spectral resolution [8] and another having lower resolution of the type described in [9]. Owing to the low sensitivity of the high-resolution spectrometer, only

the spectra from the lower-resolution spectrometer are presented here. This spectrometer had the ability to resolve the K-shell spectral features from the irradiated and spectator wire materials.

The spectrometer had a cylindrically bent quartz (101) crystal in the Cauchois optical configuration, and the spectral lines from an extended target were focused on the Rowland circle (RC) having 254 mm diameter [9]. On each laser shot, the time integrated spectra were recorded on two image plates, one on the RC where the spectral resolution is determined by the image plate spatial resolution and another 200 mm behind the RC where the resolution is enhanced by larger dispersion and is limited by the source size [9,10]. Example spectra recorded by the front and rear image plates are shown in Fig. 3. The front spectrum has lower spectral resolution and higher signal level, and the rear spectrum has higher resolution (the $K\alpha_1$ and $K\alpha_2$ lines are well resolved) and lower signal level.

The primary experimental results are the ratios of the emissions from the vertical and horizontal spectator wires and the central irradiated wire, and how these ratios are related to the numbers of energetic electrons propagating into the vertical and horizontal wires from the focal spot on the irradiated wire. The spectator wires were Gd and Dy and the central irradiated wire was Ag, Ho, or Hf. Since Gd and Dy have similar atomic numbers and have similar material properties, for a given electron energy the probabilities of 1s vacancy creation and $K\alpha$ photon generation in these two materials are practically equal, and the ratio of the emissions from the Gd and Dy spectator wires is independent of the experimental conditions such as the laser pulse energy and the position of the focal spot on the central wire. The irradiated wire materials were chosen to

represent a range of atomic numbers, from 47 (Ag) to 72 (Hf), for the purpose of studying the dependence of the energetic electrons generated in the focal spot on the atomic number of the irradiated material.

As shown in Fig. 3, two Gaussian curves representing the $K\alpha_1$ and $K\alpha_2$ lines were fitted to the $K\alpha$ spectral feature of each of the three elements (one irradiated element and two spectator elements) by the least squares technique. For each $K\alpha$ feature, the $K\alpha_1$ and $K\alpha_2$ components were assumed to have the theoretical relative intensities and energy separation. Because the instrumental broadening is practically the same for the closely-spaced line pair, the two Gaussian components were assumed to have the same line width. A linear background was fitted to each line pair, and the areas above the background and under the two Gaussian curves were calculated. Thus the number of variables for fitting the two Gaussians to each line pair was five: intensity, energy, line width, and two variables for the background.

For each element, the areas under the two Gaussian curves were added, and the ratios of the three summed areas were compared in both the front and rear spectra. It was found that the corresponding ratios in the front and rear spectra agreed to within 10%. For example, the ratios of the summed $K\alpha_1$ and $K\alpha_2$ lines of Hf, Dy, and Gd in the spectrum of Fig. 3 is 1:0.22:0.20 in the rear image plate spectrum and 1:0.21:0.21 in the front image plate spectrum.

In order to investigate possible effects that depend on the rotation of the target, such as orienting the vertical wires to be parallel to the polarization of the laser beam and orientating the target face to be perpendicular to the laser beam, spectra were recorded with the orientation of the vertical and horizontal wires rotated by 90° as shown in Fig. 4.

That is, spectra were recorded with the Gd wires vertical and the Dy wires horizontal, and other spectra were recorded with the target rotated by 90° so that the Dy wires were vertical and the Gd wires were horizontal. It was found that the emission from the vertical wires was systematically stronger than the emission from the horizontal wires. For example, shown in Fig. 5 are spectra recorded on two laser shots with (a) the Gd wires vertical and the Dy wires horizontal and (b) the Dy wires vertical and the Gd wires horizontal. For both shots, the central irradiated wire is Ho and the gap between the central and spectator wires is zero (the four spectator wires are in physical contact with the central wire). The emission from the irradiated Ho wire is practically the same on the two laser shots, and the emission from the vertical wires is stronger in both target rotational orientations.

In order to relate the $K\alpha$ emission to the energetic electron fluence from the focal spot, a model for the 1s vacancy and $K\alpha$ emission is necessary. The model should account for the material-dependent cross section for 1s vacancy creation and the fluorescence yield for $K\alpha$ emission. Since the ratios of the $K\alpha$ emissions are the primary observables of the experiment, the model does not need to account for the material-independent factors such as the laser pulse parameters that tend to cancel out in the ratios. While a Monte Carlo code could produce detailed simulations of the experimental data, the basic physics of the experiment are best understood using an analytical model. Such analytical models have proved successful in interpreting previous experimental data on the propagation of energetic electrons from irradiated materials into spectator materials at the Titan [7] and LULI [6,11,12] laser facilities.

For a given electron energy, the probability for the creation of a 1s vacancy and the emission of a $K\alpha$ photon per unit path length is proportional to the product $\sigma\rho f/A$ where σ is the cross section for 1s vacancy creation, ρ is the material density, f is the fluorescence yield, and A is the atomic number. Multiplying by the electron range in the material and the photon escape probability gives the number of photons generated by the energetic electron, and multiplying by the spectrometer throughput gives the detected intensity of $K\alpha$ photons. The expression for the relative number of detected $K\alpha$ photons generated per energetic electron propagating in a spectator or irradiated wire material is $\sigma\rho fRT\varepsilon/A$ where R is the electron range, T is the photon escape factor, and ε is the spectrometer throughput. The electron range is calculated using the NIST ESTAR continuous slowing down model [13], and the transmittance of the $K\alpha$ photons is calculated using the NIST attenuation database [14]. The spectrometer throughput uses the measured integrated reflectivity of the quartz (101) crystal [15].

Previous experiments indicated that the energies of the electrons propagating from the focal spot into surrounding materials were in the range 0.4 MeV to 1 MeV [6,11,12]. For the present experiment, we use the typical value 0.7 MeV to calculate the electron range. Changes in the assumed electron energy have a small effect on the ratios of the photons emitted from the various wire materials. We assume the photons pass through 0.25 mm of material which is equal to the spectator wire radius and is approximately equal to half the electron range in the irradiated wire materials. Once again, different attenuation depths have a small effect on the detected photon ratios. In particular, the produce RT varies slowly with the assumed electron energy, even over the rather wide range of irradiated wire materials from Ag to Hf, because the range R into the

material increases with energy and the escape factor T decreases with depth into the material.

When the propagating electron energy is much greater than the ionization potential of the 1s electron in the spectator or irradiated wire material, as is the case here, the cross section σ for 1s vacancy creation is practically independent of the electron energy and is proportional to $(Ry/P)^2$ where Ry is the Rydberg constant (13.6 eV) and P is the 1s ionization potential [16]. Substituting values into the expression $\sigma \rho f R T \epsilon / A$ and normalizing to the result for Dy, the relative numbers of detected $K\alpha$ photons per energetic electron propagating in Ag, Gd, Dy, Ho, and Hf are 1.14:1.29:1:0.79:0.41. These factors are used to scale the relative $K\alpha$ signal levels, as measured by areas of the two Gaussians fitted to each $K\alpha$ feature, and to determine the relative numbers of energetic electrons propagating in the spectator and irradiated wire materials.

Shown in Fig. 6 for each laser shot is the ratio of the electrons propagating in (a) the horizontal spectator wires and the irradiated wire, (b) the vertical spectator wires and the irradiated wire, and (c) the vertical and horizontal spectator wires. The ratios are plotted as functions of the distance from the center of the irradiated wire to the surface of the spectator wire facing the irradiated wire, which is equal to the separation gap (0, 0.4 mm, or 0.8 mm) plus the 0.25 mm radius of the irradiated wire. For all shots, the spectator wires were Gd and Dy with either the Gd wire vertical or rotated by 90° with the Dy wire vertical. The irradiated wires were Ag (diamond data symbols), Ho (triangle data symbols), or Hf (square data symbols). In Fig. 6(a) and (b), the spectator to irradiated ratios are on a log-log plot, and a straight line is fitted to the data points using the least squares technique. The slopes of the straight lines on the log-log plots indicate

that the horizontal wire to irradiated wire electron number ratio shown in Fig. 6(a) decreases with distance to the power -1.58 with one-sigma uncertainty ± 0.04 . The vertical to irradiated electron number ratio shown in Fig. 6(b) decreases with power -1.16 ± 0.06 . Thus the vertical to irradiated ratio decreases significantly more slowly with distance compared to the horizontal to irradiated ratio. This indicates that the cone of energetic electrons propagating from the focal spot toward the vertical wires has a significantly smaller angle than the cone of electrons propagating toward the horizontal wires, and this implies that energetic electrons are selectively driven in the (vertical) polarization direction of the incident laser beam than in the perpendicular direction.

Shown in Fig. 6(c) are the ratios of the electrons propagating in the vertical and horizontal wires as functions of distance from the focal spot, and a straight line was fitted to the data points. The vertical to horizontal ratio doubles over a distance of 0.85 mm, and once again this implies that energetic electrons are selectively driven in the (vertical) polarization direction than in the perpendicular direction

III. Discussion

Based on prior experiments on the propagation of energetic electrons from the focal spot of an intense laser pulse, targets were designed for the quantitative study of energetic electrons driven in the polarization direction of the incident laser beam. The target design, experimental technique, and data analysis were chosen to mitigate laser shot-to-shot variations and other experimental uncertainties. The primary observables are the ratios of the $K\alpha$ emissions from the three wire materials: the central irradiated wire, the two vertical wires in the polarization direction, and the two horizontal wires in the perpendicular direction. The emissions from the two vertical wires are summed as are the

emissions from the two horizontal wires, and this mitigates small mis-positioning of the focal spot on the central wire. In addition, when using the analytical model to calculate the ratios of the $K\alpha$ emission generated by energetic electrons propagating through the three wire materials, the material properties tend to be similar and to cancel when taking the ratios. For example, the energetic electron ranges depend primarily on the electron density in the metallic wires which are well known, and the ratio of the ranges changes slowly with the assumed electron energy. Finally, the target was rotated by 90° on different laser shots so that the vertical and horizontal wire materials were interchanged, and the results were the same: the emission from the vertical wires was systematically stronger than from the horizontal wires. Moreover, the ratio of the vertical to horizontal emission increases with distance from the focal spot as indicated in Fig. 6(c), and this implies that the energetic electrons propagating in the vertical (polarization) direction have a smaller cone angle than those propagating in the horizontal direction, perpendicular to the polarization. The conclusion is that energetic electrons are selectively driven in the polarization direction of the oscillating electric field of the normally-incident laser beam, and this is consistent with the multiphoton inverse Bremsstrahlung absorption process.

While the changes in the emission ratios shown in Fig. 6 are readily apparent, the scatter in the data points could be reduced by several experimental improvements. For example, possible small-angle scattering of the energetic electrons as they propagate from the focal spot to the edge of the irradiated wire would tend to smear out the smaller propagation cone angle in the polarization direction and the larger cone angle in the perpendicular direction, and this effect can be reduced by making the irradiated wire

diameter smaller such as 0.25 mm rather than the 0.5 mm diameter used in the present experiment. Similarly, the sampling of the cone angle of the energetic electrons propagating toward the spectator wires would be improved by using a smaller spectator wire diameter such as 0.25 mm rather than 0.5 mm. Finally, having more gap separations than the three used here (0, 0.4 mm, and 0.8 mm) would better characterize the ratio curves shown in Fig. 6.

Acknowledgements. This work was funded by the Defense Threat Reduction Agency, grant number DTRA-1-10-0077 and by the NNSA-DS and SC-OFES Joint Program in High-Energy-Density Laboratory Plasmas, grant number DE-NA0001840. Prepared by LLNL under Contract DE-AC52-07NA27344.

References

1. J. H. Eberly in Progress in Optics, edited by E. Wolf (John Wiley, New York, 1969), vol. VII.
2. V. P. Silin, Zh. Eksperm. i Teor. Fiz. **47**, 2254 (1964). Translation: Sov. Phys. JETP **20**, 1510 (1965).
3. J. F. Seely and E. G. Harris, Phys. Rev. A **7**, 1064 (1973).
4. J. F. Seely in Laser Interaction and Related Plasma Phenomena, edited by H. Hora (Plenum Press, 1974), vol. 3.
5. P. Gibbon, Short Pulse Laser Interactions with Matter (Imperial College Press, 2005).
6. J. F. Seely, C. I. Szabo, P. Audebert, and E. Brambrink, Phys. Plasmas **18**, 062702 (2011).
7. C. A. Di Stefano *et al.*, Phys. Plasmas (submitted for publication).
8. J. F. Seely *et al.*, Rev. Sci. Instr. **85**, 11D618 (2014).
9. J. F. Seely, C. I. Szabo, U. Feldman, L. T. Hudson, A. Henins, P. Audebert, and E. Brambrink, Rev. Sci. Instru. **81**, 10E301 (2010).
10. J. F. Seely, L. T. Hudson, G. E. Holland, and A. Henins, Appl. Opt. **47**, 2767 (2008).
11. J. Seely *et al.*, High Energy Density Phys. **5**, 263 (2009).
12. J. F. Seely, C. I. Szabo, P. Audebert, E. Brambrink, E. Tabakhoft, and L. T. Hudson, Phys. Plasmas **17**, 023102 (2010).
13. <http://physics.nist.gov/PhysRefData/Star/Text/ESTAR.html>
14. <http://www.nist.gov/pml/data/ffast/index.cfm>
15. C. Szabo, U. Feldman, S. Seltzer, L. T. Hudson, M. O'Brien, H.-S. Park, and J. F. Seely, Opt. Letters **36**, 1335 (2011).

16. C. Hombourger, J. Phys. B **31**, 3693 (1998).

Figure Captions

Fig. 1. [\(Color online\)](#) Schematic of the multiphoton inverse Bremsstrahlung absorption (MIBA) process where an electron oscillating in the electric field E of an intense laser beam absorbs multiple photons during a collision with a nucleus having charge Z and propagates in the polarization direction with relativistic energy.

Fig. 2. [\(Color online\)](#) The target showing the central irradiated wire, vertical wires in the direction of the polarization of the incident laser beam, and the horizontal wires in the perpendicular direction.

Fig. 3. Spectra from (a) the rear image plate and (b) the front image plate showing the fit of two Gaussian curves to each of the three $K\alpha$ features from the Hf irradiated wire and the Gd and Dy spectator wires.

Fig. 4. [\(Color online\)](#) The two orthogonal orientations of the target with the vertical and horizontal wire materials reversed. The polarization of the incident laser beam is indicated by the vertical arrows.

Fig. 5. The spectra from two laser shots with (a) the Gd wires vertical and the Dy wires horizontal and (b) the Dy wires vertical and the Gd wires horizontal.

Fig. 6. (a) The ratios of the electrons driven into (a) the horizontal and irradiated wires, (b) the vertical and irradiated wires, and (c) the vertical and horizontal wires.

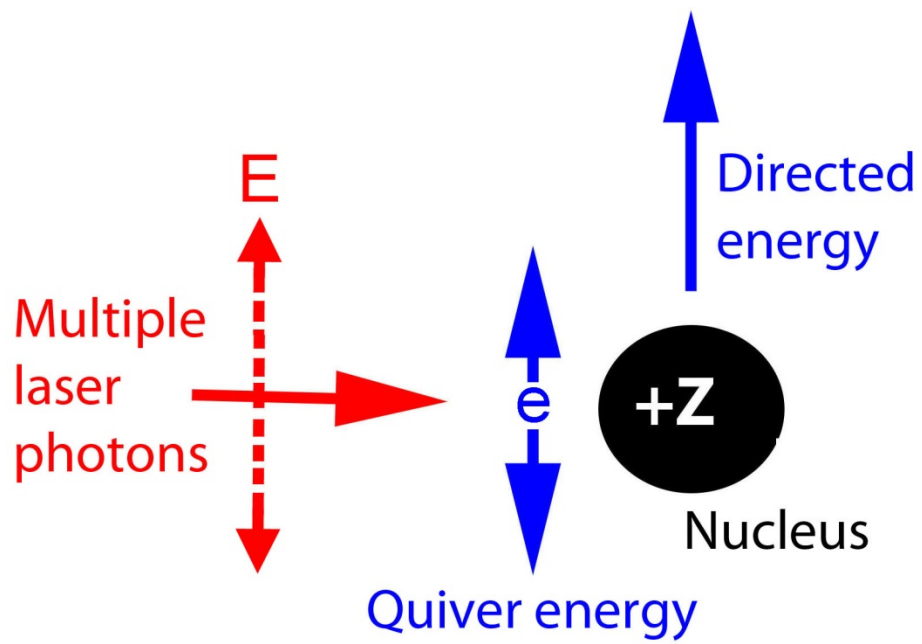


Figure 1

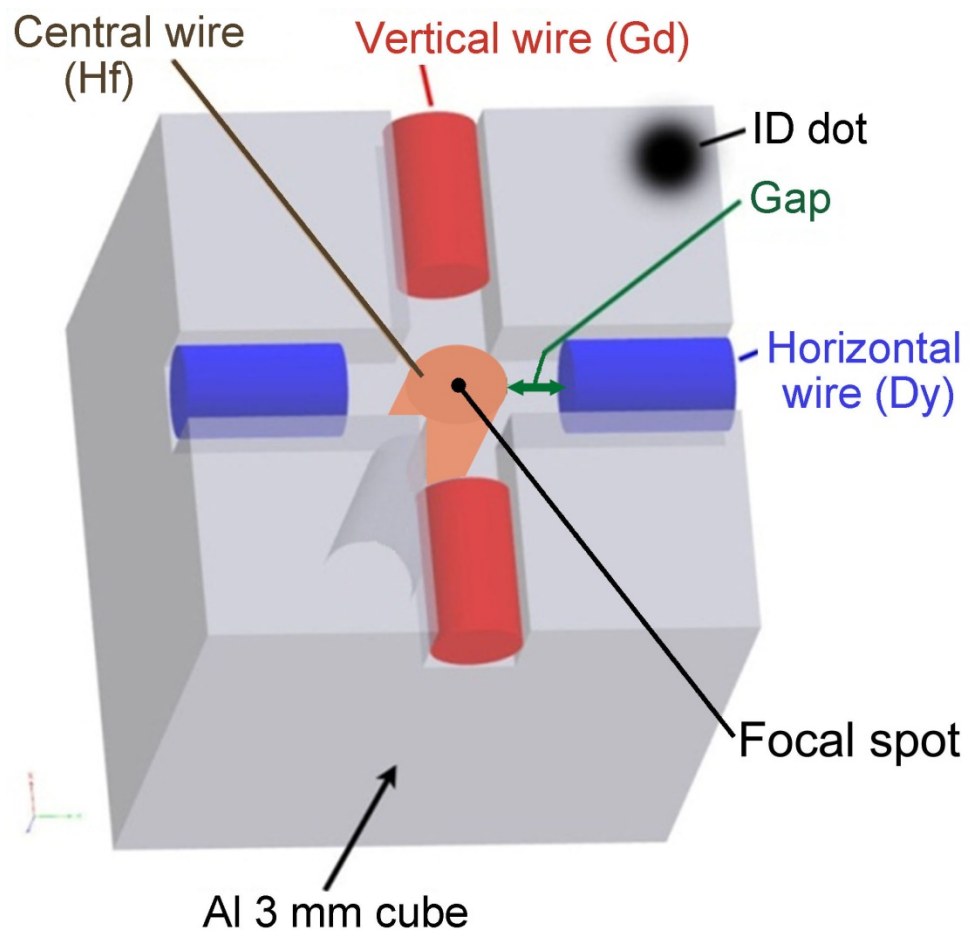


Figure 2

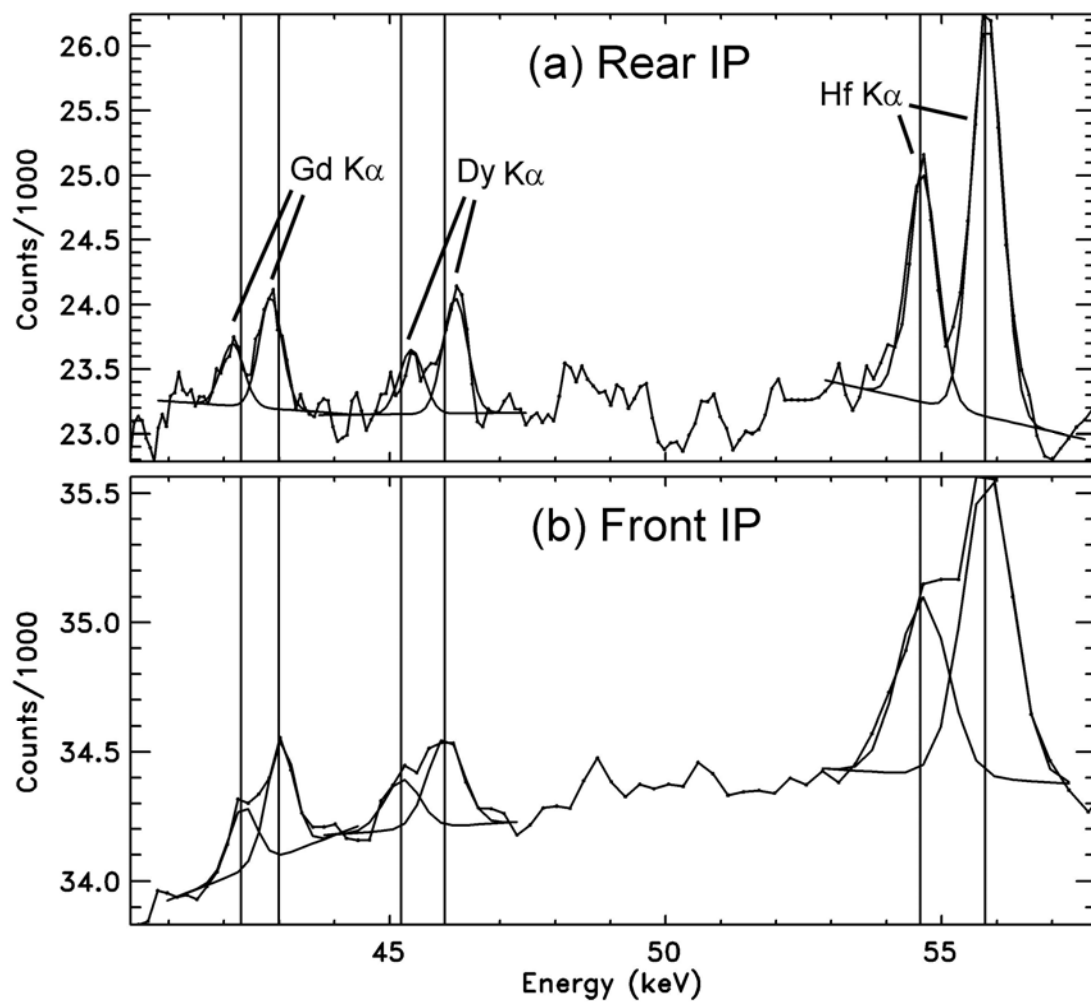
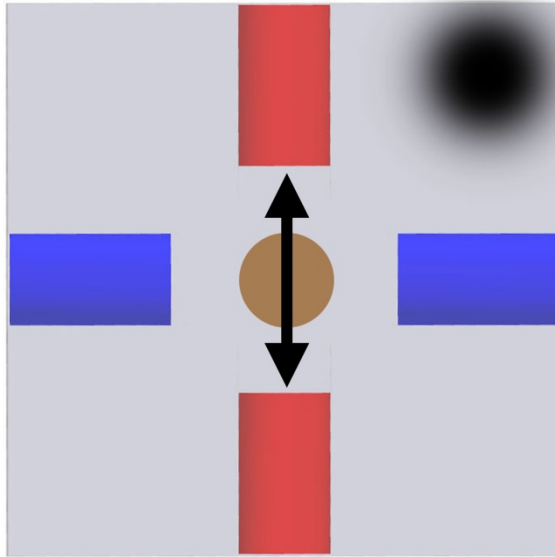


Figure 3

(a)



(b)

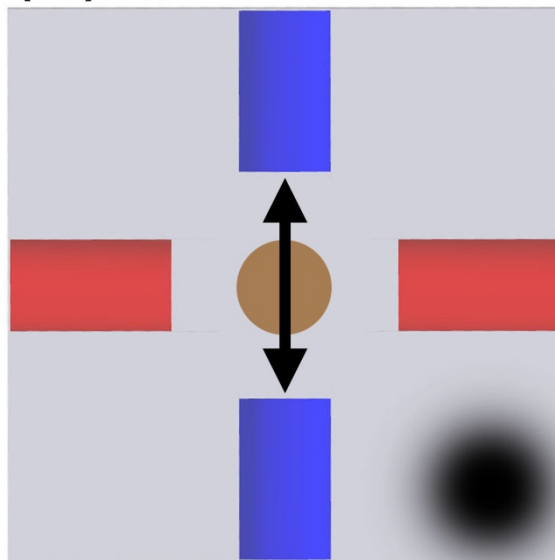


Figure 4

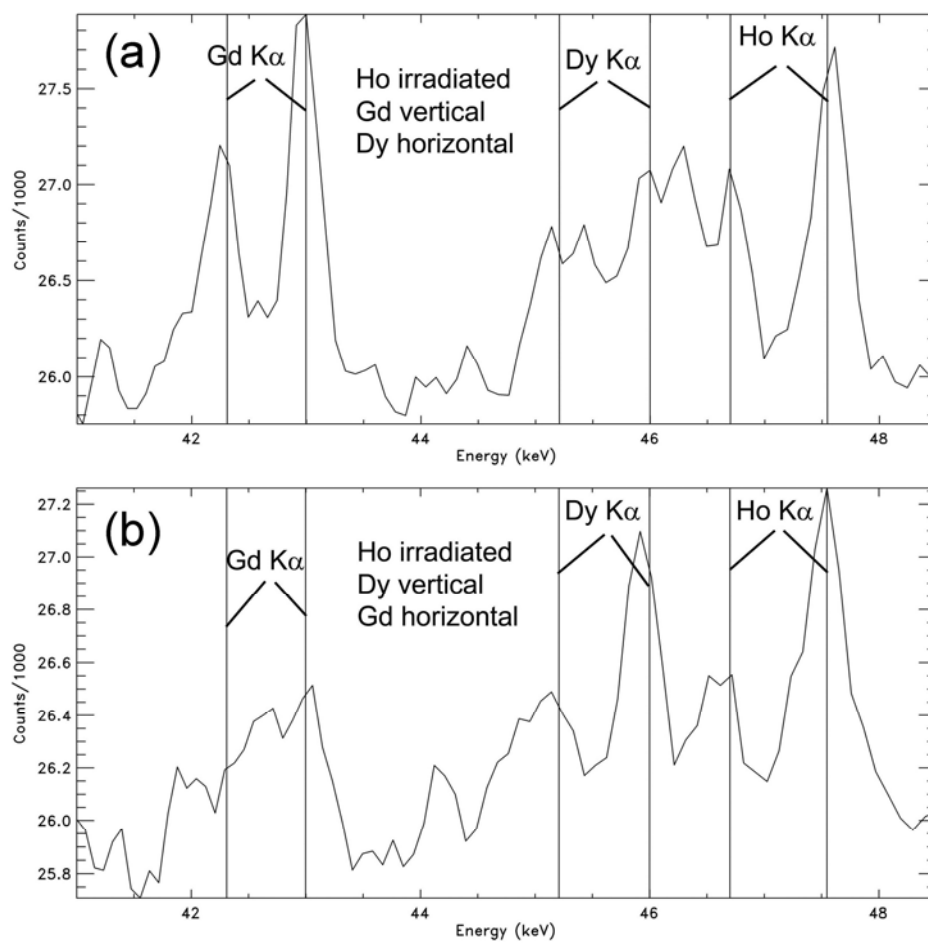


Figure 5

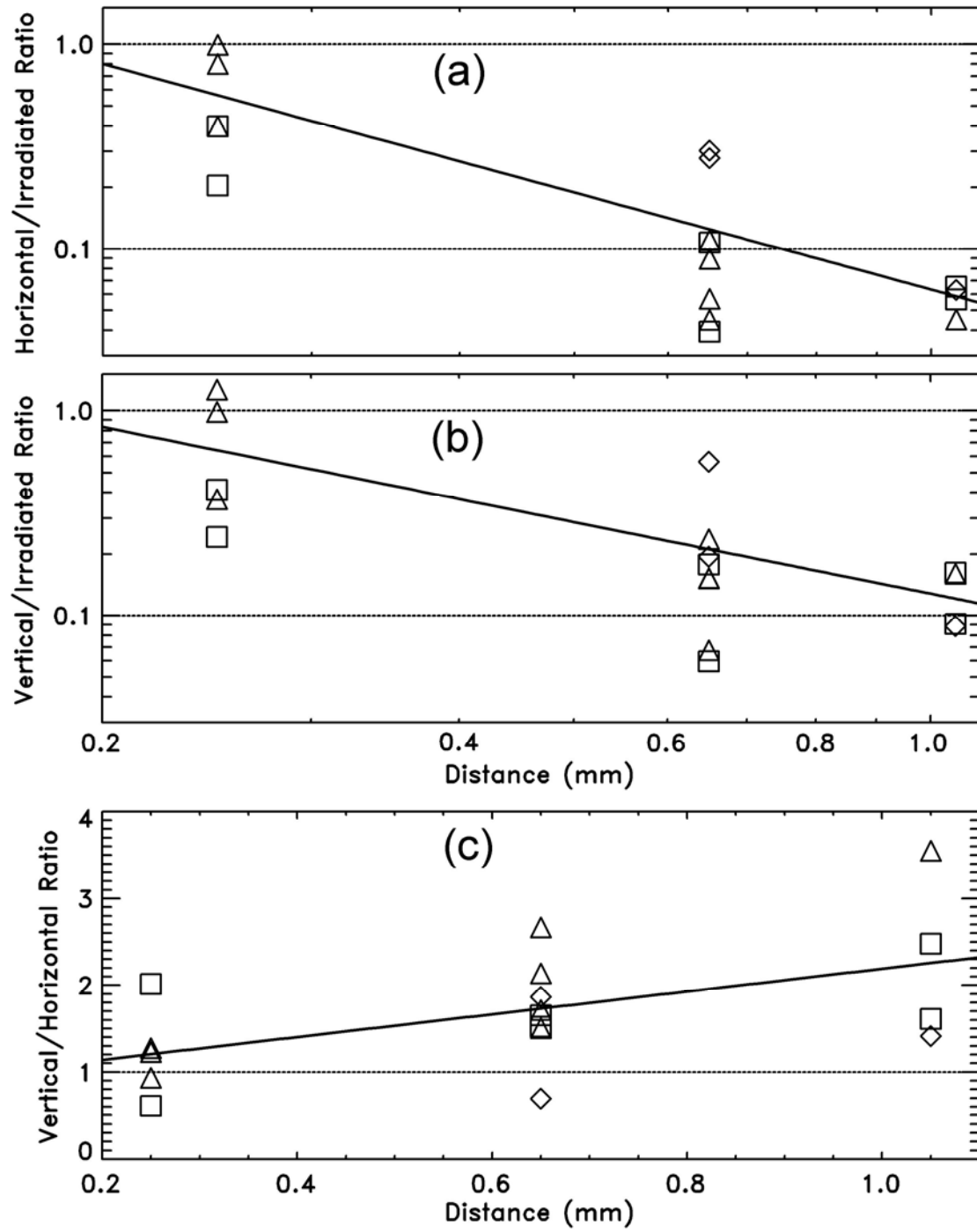


Figure 6